# Synthesis and Characterization of Flame Retarding UV-Curable Organic–Inorganic Hybrid Coatings

**Sevim Karataş,[1] Zuhal Hoşgör,[1] Yusuf Menceloğlu,[2] Nilhan Kayaman-Apohan,[1] Atilla Güngör[1]**

[1]*Department of Chemistry, Faculty of Art and Science, Marmara University, 34722 Göztepe, Kadikoy-Istanbul, Turkey*
[2]*Faculty of Engineering and Natural Sciences, Sabancı University, 34956 Tuzla-Istanbul, Turkey*

Received 31 August 2005; accepted 17 January 2006
DOI 10.1002/app.24274
Published online in Wiley InterScience (www.interscience.wiley.com).

**ABSTRACT:** UV-curable, organic–inorganic hybrid materials were synthesized via sol–gel reactions for tetraethylorthosilicate, and methacryloxypropyl trimethoxysilane in the presence of the acrylated phenylphosphine oxide resin (APPO) and a bisphenol-A-based epoxy acrylate resin. The sol–gel precursor content in the hybrid coatings was varied from 0 to 30 wt %. The adhesion, flexibility, and hardness of the coatings were characterized. The influences of the amounts of inorganic component incorporated into the coatings were studied. Results from the mechanical measurements show that the properties of hybrid coatings improve with the increase in sol–gel precursor content. In addition, thermal properties of the hybrids were studied by thermogravimetric analysis in air atmosphere. The char yield of pure organic coating was 32% and that of 30 wt % silicate containing hybrid coating was 30% at 500°C in air atmosphere. This result demonstrates the pronounced effect of APPO on the flame retardance of coatings. Gas chromatography/mass spectrometry analyses showed that the initial weight loss obtained in thermogravimetric analysis is due to the degradation products of the photoinitator and the reactive diluent. © 2006 Wiley Periodicals, Inc. J Appl Polym Sci 102: 1906–1914, 2006

**Key words:** UV-curable coatings; sol–gel materials; nanocomposite; organic–inorganic hybrids; flame resistance

## INTRODUCTION

In recent years, the synthesis and characterization of organic–inorganic hybrid materials by the sol–gel process have received considerable attention.[1–4] The hybrid materials obtained possess unique property combinations of the inorganic (hard and brittle) and the organic (soft and flexible), while maintaining optical transparency.[5,6] Most organic–inorganic hybrid network materials reported in literature are thermally cured.[7,8] Alternatively, hybrid materials can be prepared by the use of radiation curing using an UV curable binder system.[9–11] Hydrolysis and condensation reactions of the inorganic part and photopolymerization of the organic moieties lead to a glass-like material at room temperature. In these networks, it is thought that the Si—O—Si inorganic backbone structure provides high abrasion resistance, high modulus, and thermal stability. The organic part of the network contributes properties such as impact, toughness, and adhesion improvement. Hybrid materials have a huge potential for applications in a variety of advanced technologies both as structural materials (matrices for HP composites) and functional materials (catalyst supports, biosensors, and active glasses).[12,13] However, the main commercial applications, at present, are in the field of protective coatings of both inorganic and organic substrates.

Up to now, several organic–inorganic coating materials have been described. Bosch et al. have studied the photoinitiated polymerization of HEMA inside the sol–gel glass and the material obtained was homogeneous and transparent with a wide range of HEMA content.[14] Zhang et al. reported the synthesis of organic–inorganic hybrid network material based on a UV curable epoxy acrylate resin.[15] It was found that the thermal stability of the hybrids could be improved with increasing silica content. The products show enhanced hardness, flexibility, and impact strength over a pure organic coating system. Hsiue et al. synthesized the copolymer of styrene and 3-(trimethoxysilyl)propyl methacrylate.[16] After curing, the hybrid copolymers possessed excellent miscibility; however, thermally unstable silyl ester groups that were formed during heat treatment reduced the stability of hybrid copolymer. Wouters et al. have studied the preparation of an hybrid network based on UV-curable acrylate end-capped polyurethane resins incorporated in an inorganic network, while maintaining optical clarity.[17] By adding an intrinsically conductive polymer, the coatings became antistatic without significant loss of their transparency. Messori et al. reported the application

*Correspondence to:* A. Güngör (atillag@marmara.edu.tr).
Contract grant sponsor: Commission of Scientific Research Project, Marmara University; contract grant number: FEN-043/030303.

of α- and α,ω-triethoxysilane-terminated poly(ε-caprolactone) containing hybrid materials as protective coatings on PMMA substrates and the evaluation of their effect on flame resistance.[18] For all coated samples, a very sharp increase of flame resistance was striking evidence with respect to uncoated PMMA.

This work demonstrates that the preparation of organic–inorganic hybrid networks based on UV-curable acrylate functionalized 2,2-bis(4-β-hydroxy ethoxy phenyl)phenyl phosphine oxide resin. The hybrid materials are characterized by the analysis of various properties such as hardness, impact resistance, gloss, flexibility, and crosscut adhesion. The improvement of flame resistance of protective coatings also represents an important industrial goal. Therefore, the hybrid coatings were also evaluated with respect to their thermo-oxidative stability.

## EXPERIMENTAL

### Materials

*p*-Bromo fluoro benzene (Acros Organics, Istanbul, Turkey), dichloro phenylphosphineoxide (Merck, Istanbul, Turkey), magnesium (Riedel-de Haen, Istanbul, Turkey), ethylene carbonate (Riedel-de Haen), sodium carbonate (Merck), acryloyl chloride (Merck), triethylamine (Fluka, Istanbul, Turkey), and potassium hydroxide (Merck) were used without further purification. The bisphenol-A-based epoxy acrylate (EA) was previously synthesized in our laboratory.[12] *N*-vinyl-2-pyrrolidone (NVP) was provided by ISP, Turkey. Tetraethylorthosilicate (TEOS) and methacryloxypropyl trimethoxysilane (MAPTMS) were kindly supplied by Wacker. Surface wetting additive (DC-190 silicon glycol copolymer, Wacker, Turkey) was provided by Dow Chemicals, Turkey. 1-Hydroxy cyclohexyl phenyl ketone (Irgacure 184) was supplied by Ciba Specialty Chemicals (PI). All materials were used as received. Anode oxidized aluminum panels (AlMg1) were used in all samples ($75 \times 150 \times 0.82$ mm$^3$). In this procedure, an oxide film was produced on aluminum metal by electrolysis. The metal to be treated is made the anode in an electrolytic cell and its surface is electrochemically oxidized. Anodization can improve surface properties and appearance.

### Characterization

The chemical structures were identified by FTIR and NMR spectra.

FTIR spectra were recorded on Shimadzu 8303 FTIR Spectrometer. $^1$H NMR spectra were obtained by using Varian model T-60 NMR spectrometer operated at 200 MHz.

To evaluate the coating properties of crosslinked films, the coatings were cast on aluminum panels using a 60 μm applicator and cured in a bench type UV processor produced by EMA Group (120 W/cm medium pressure mercury UV lamps).

The solid state Si-cross-polarization (CP)/magic-angle-spinning (MAS) NMR spectra were recorded using a Varian Unity Inova spectrometer operated at 500 MHz.

The ATIR measurements were performed on Bruker Equinox 55 Spectrometer.

The film properties were measured in accordance with the corresponding standard test methods as indicated. These include the thickness (ASTM D-1186), gloss (ASTM D-523-80), crosscut adhesion (DIN 53151), pendulum hardness (DIN 53157), impact resistance (ASTM D-2794-82), Erichsen cupping test (DIN 53156).

Thermogravimetric analyses (TGA) of the UV-cured free films were performed using a NETZSCH STA 449 C model TGA. Samples were run from 30 to 750°C with a heating rate 10°C/min under air atmosphere.

GC-MS analyses of hybrid films were obtained by Thermo Finnigan Trace GC Ultra and Thermo DSQ.

### Synthesis of bis[(4-β-hydroxyethoxy)phenyl]phenyl phosphineoxide

The synthesis of bis(4-fluorophenyl)phenyl phosphineoxide (BFPPO), by a variation of known Grignard technique, has been described in detail elsewhere.[19] 4,4′-Bis(hydroxyphenyl)phenyl phosphineoxide (BHPPO) was prepared by hydrolyzing BFPPO using potassium hydroxide. Then the product was purified using fractional recrystallization from a 20% solution of methanol/water.[20] BHEPPO was synthesized by the reactions of BHPPO with ethylene carbonate according to literature.[21] Briefly, a spherical flask (500 mL), equipped with a reflux condenser, stirrer, thermometer, and nitrogen inlet, was charged with BHPPO (5 g, 0.016 mol), ethylene carbonate (2.8 g, 0.032 mol), and sodium carbonate (0.016 g) as catalyst. The mixture was heated to 165–170°C under nitrogen for 2 h. The crude product was washed with water several times to remove unreacted ethylene carbonate and recrytallized from methanol. A light brown glassy product was obtained in a yield about 90%.

### Synthesis of acrylated phenyl phosphine oxide oligomer

BHEPPO (5.8 g; 0.015 mol) dissolved in dichloromethane was charged into a three-necked flask, equipped with a stirrer, a thermometer, a dropping funnel, and a condenser. Five milliliters of triethylamine was added and the system was cooled to 0°C in an ice bath. Acryloyl chloride weighing 3.28 g (0.036 mol, 3 mL) was slowly dropped into the flask and the mixture was reacted at 0°C for 4 h. The solution was microfiltered to remove triethylamine hydrochloride. The filtrate was washed with aqueous sodium car-

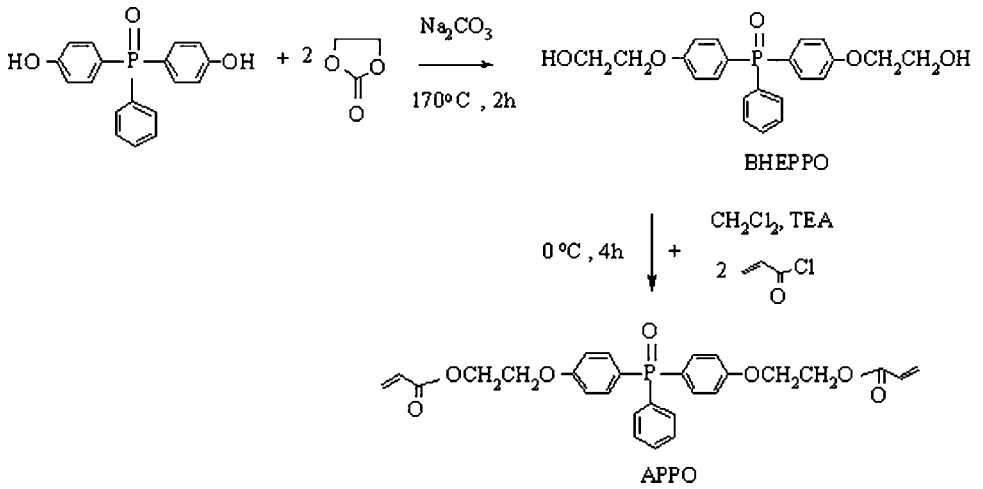


**Scheme 1** Synthesis of bis[(4-β-hydroxyethoxy)phenyl]phenyl phosphineoxide (BHEPPO) and acrylated phenyl phosphine oxide oligomer (APPO).

bonate and water respectively, to remove traces of HCl and to neutralize the system. Then the filtrate was dried with anhydrous $Na_2SO_4$. The solvent was evaporated off under vacuum and a clear, viscous product was obtained (yield: 90%). A representation of this reaction is shown in Scheme 1.

### Preparation of hybrid sol–gel material

The coatings were prepared starting from a mixture of acrylates (component A) and a mixture of organosilanes (components B).

Component A is composed of acrylated phenyl phosphine oxide oligomer, a bisphenol-A epoxy acrylate (EA), *N*-vinylpyrrolidone (NVP), the photoinitator (PI), and surface wetting agent (DC-190).

Component B is composed of a hydrolysis mixture of methacryloxy propyl trimethoxysilane (MAPTMS) (5 g, 0.02 mol), tetraethylorthosilicate (TEOS) (2.1 g, 0.01 mol). MAPTMS and TEOS were allowed to hydrolyze partially in water (0.9 g, 0.05 mol). To prevent the corrosiveness of the residual acid on aluminum substrates, hydrolysis was performed without using any catalyst. After stirring for 2 h, the mixture was allowed to age for 48 h under sealed condition in dark.

In all, five samples were prepared and characterized. The composition of reaction mixtures is given in Table I.

After homogenization, the formulations were cast on to aluminum panels using a wire-gauged bar applicator obtaining a layer thickness of 60 μm. The applied coatings were hardened by a UV processor houses a medium pressure mercury lamp (120 W/cm) situated 15 cm above the moving belt after six pass. The speed of the processor is 2 m/min. Moreover, hybrid free films were prepared by pouring the viscous liquid formulations on to a Teflon™-coated mold. To prevent the inhibiting effect of oxygen, resin in the mold was covered by transparent, 100 μm thick Teflon film before irradiation with a high pressure UV-lamp (OSRAM, 300W), a quartz glass plate was placed over the teflon film to obtain a smooth surface. After 150 s irradiation under UV-lamp, a 200 μm thick hybrid free films were obtained.

## RESULTS AND DISCUSSION

The flame retardance properties of coatings are very important whatever the application might be. This work focused on further improvements of the flame retardancy of hybrid coatings via incorporation of phosphorous containing UV-curable oligomers into the sol–gel matrix. For this purpose, acrylate functional phenyl phosphineoxide resin was synthesized. Scheme 1 depicts the synthesis routes of the oligomer (APPO). Firstly, bis[(4-β-hydroxyethoxy)-phenyl]phenyl phosphineoxide (BHEPPO) was obtained. Then, the acrylated oligomer was synthesized by the reaction of acryloyl chloride and triethyl amine. The chemical structures of the resulting compounds were characterized by FTIR and $^1$H NMR. Figure 1 displays the FTIR spectra of APPO and its precursors BFPPO and BHPPO. Peak appearing at

**TABLE I**
**Compositions of Hybrid Materials**

| | Component A | | | | | |
|---|---|---|---|---|---|---|
| Sample name | APPO (g) | EA (g) | NVP (g) | PI (g) | DC190 (g) | Component B (wt %) |
| Control | 1 | 1 | 1.86 | 0.12 | 0.02 | 0 |
| PPCH1 | 1 | 1 | 1.86 | 0.12 | 0.02 | 5 |
| PPCH2 | 1 | 1 | 1.86 | 0.12 | 0.02 | 10 |
| PPCH3 | 1 | 1 | 1.86 | 0.12 | 0.02 | 20 |
| PPCH4 | 1 | 1 | 1.86 | 0.12 | 0.02 | 30 |

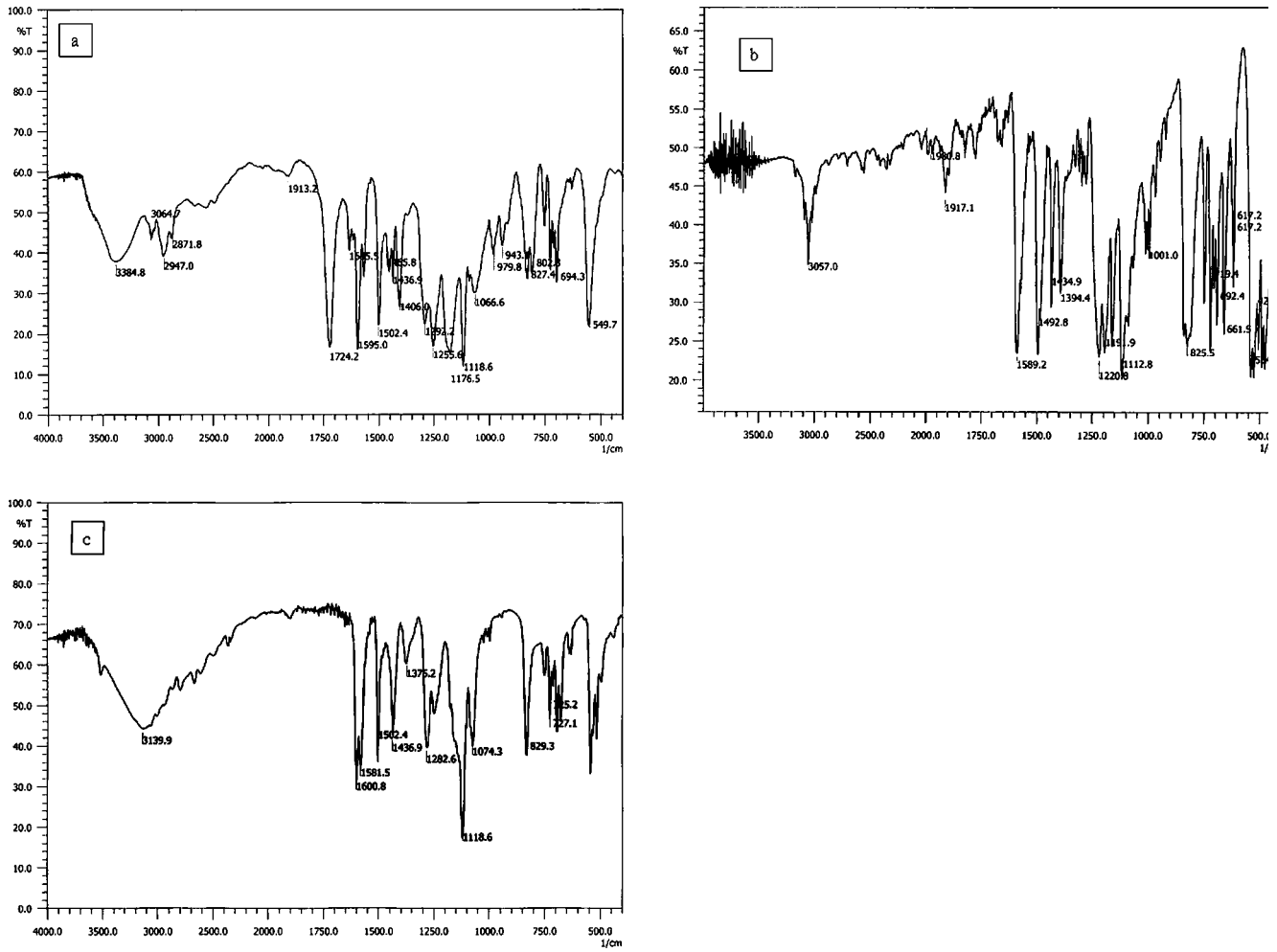


**Figure 1** FTIR spectra of (a) APPO, (b) BFPPO, (c) BHPPO.

1221 $cm^{-1}$ for BFPPO's IR indicates the existence of fluorine groups. Other peaks at 1191 $cm^{-1}$ (P=O), 1435 $cm^{-1}$ (P—Ph), 1589 $cm^{-1}$ (C=C), 3057 $cm^{-1}$ (aromatic C—H str.) confirm the aromatic phosphineoxide structure of BFPPO [Fig. 1(a)]. After hydrolysis, the formation of hydroxyl groups was demonstrated by broad absorption band at 3138 $cm^{-1}$. The fluorine group's characteristic absorption also emerged [Fig. 1(b)]. Moreover, the absorption band related to acrylate groups at 1724 $cm^{-1}$ (C=O str.) confirms the formation of expected structure.

The final product was further characterized by $^1H$ NMR. Figure 2 shows the $^1H$ NMR spectrum of APPO. The chemical shifts appearing between 7.4 and 7.8 ppm (O=P—$C_6H_5$) and 7.0 ppm (—O—$C_6H_4$—P=O) can be associated to the aromatic protons in APPO. The three olefinic protons of the acrylate functionality form a complex higher order in the range of 5.7–6.4 ppm. It is known that, upon polymerization, the olefinic protons are converted into aliphatic methylene and methine groups and appear at much higher field. The peaks observed between 1.3 and 2.8 ppm may be due to this undesirable polymerization with negligible conversion. The methylene groups that are bounded to the oxygen atom and acrylate group appear at 4.2 and 4.5 ppm as triplets, respectively.

Organic–inorganic hybrid free films and coatings on aluminum panels were prepared by sol–gel method. Inorganic part of the hybrid system is composed of MAPTMS and TEOS where MAPTMS acts as a coupling agent between the organic and inorganic moieties and TEOS acts as the inorganic

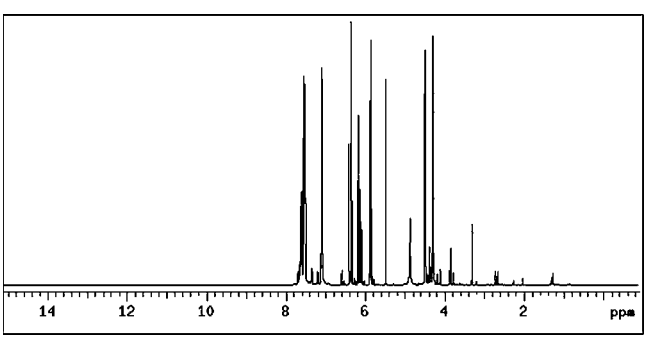


**Figure 2** $^1H$ NMR spectrum of APPO.

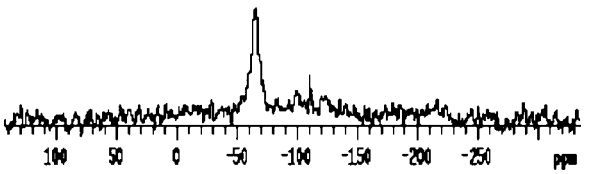


**Figure 3** Solid state $^{29}$Si NMR spectrum for 10 wt % hybrid coating.

crosslinker. Totally, at five different compositions, 20 samples were prepared and characterized.

The $^{29}$Si CP/MAS NMR spectrum of the 10 wt % of hybrid sample is shown in Figure 3 (PPCH2). Three kinds of signals were observed at −66, −100, and −110 ppm in the entire spectrum. The peak at −66 ppm is assigned to $T^3$ species [R-Si$(OSi)_3$], the −100 ppm peak to $Q^3$ species [Si$(OSi)_3$(OH)] and the −110 ppm peak to $Q^4$ species [Si$(OSi)_4$]. This result shows that the hydrolysis and condensation reactions of MAPTMS and TEOS structures have proceeded very rapidly and almost fully condensed structure was obtained.

The feed compositions and some physical characterizations of hybrid coatings are collected in Tables I and II, respectively. Each result reported in this article is an average of four separate measurements performed. All hybrid coatings showed good adhesion on aluminum panels. Hundred percent adhesion was reached at 10% sol–gel precursor content. It is obvious that, the general bulk properties of hybrid coatings depend on the structure of the organic portion, since the inorganic part is used in small portions in the coatings formulations. However, the crosscut adhesion experiments showed that the incorporation of MAPTMS and TEOS into the organic network increased the adhesion property, probably due to fact that more siloxane distributes on the substrate and produced Si—O—Al bonding.[22]

ATIR spectroscopy is a simple and useful technique to check the interaction of the alkoxysilane structure with metal and semimetal oxide surfaces. The infrared spectrum of the control sample and ATIR of corresponding coating on aluminum are given in Figures 4(a) and 4(b). It can be thought that all of the characteristic bands remain intact. The asymmetric Si—O—Si band is located at 1037 cm$^{-1}$. Other Si-related bands in this region (Si—O—Si symmetric stretching bands: 694–796 cm$^{-1}$) have not been identified due to the several peaks located in the same region coming from organic network. In recent papers, vibration band for the Al—O—Si was reported as around 750 cm$^{-1}$ with a very smooth appearance.[23,24] The ATIR spectrum of 10 wt % of hybrid coating demonstrated that this band could not be detectable because of the other peaks related to acrylated phenyl phosphine oxide resin at the same position.

Coatings gloss is a complex phenomenon resulting from the interaction between light and the surface of the coating.[25] The gloss is affected strongly by surface roughness. As can be seen in Table II, the gloss of coatings, at both 20° and 60°, increased gradually with increasing addition of the silica sol. The increased gloss may be due to more effective crosslinking via higher silicate functionality, which resulted in more uniform film surface. The surface tension of the coating formulation may also be a factor. The addition of MAPTMS and TEOS due to the increased silicate functionality reduces the surface tension of the system and the coating formulation easily spreads on the substrates.

The hardness of coating is the most important factor affecting the abrasion and scratch resistance. Hard coatings give better scratch resistance, whereas abrasion resistance is also affected by surface friction. Chain flexibility and crosslinking degree of the network plays a major role in determination of hardness. In Figure 5, pendulum hardness of organic–inorganic coatings as a function of the sol–gel precursor content is shown. As seen from figure, incorporation of MAPTMS and TEOS greatly improves the hardness, which increases with increasing amount of inorganic material. The enhance in hardness can be attributed to Si—O—Si backbone of the inorganic network formed by condensation of silicate functionalities or to enlarged inorganic clusters in the hybrid network.

Flexibility relates to the requirement that a coating should not crack under the fabrication or application caused distortion, thus the elongation at break should be greater than this extension.[25] In Table II, it

**TABLE II**
**Physical Characterizations of Hybrid Materials**

| Sample design | Thickness (μm) | Gloss | | Cross cut adhesion (%) | Erichsen cupping test (mm-axis) |
|---|---|---|---|---|---|
| | | 60° | 20° | | |
| Control | 50 | 94 ± 1 | 74 ± 1 | 95 | 2.3 ± 0.2 |
| PPCH1 | 70 | 97 ± 1 | 79 ± 1 | 95 | 2.2 ± 0.1 |
| PPCH2 | 60 | 98 ± 1 | 80 ± 2 | 100 | 1.7 ± 0.3 |
| PPCH3 | 50 | 98 ± 2 | 80 ± 2 | 100 | 1.3 ± 0.3 |
| PPCH4 | 65 | 100 ± 1 | 84 ± 1 | 100 | 1.2 ± 0.2 |

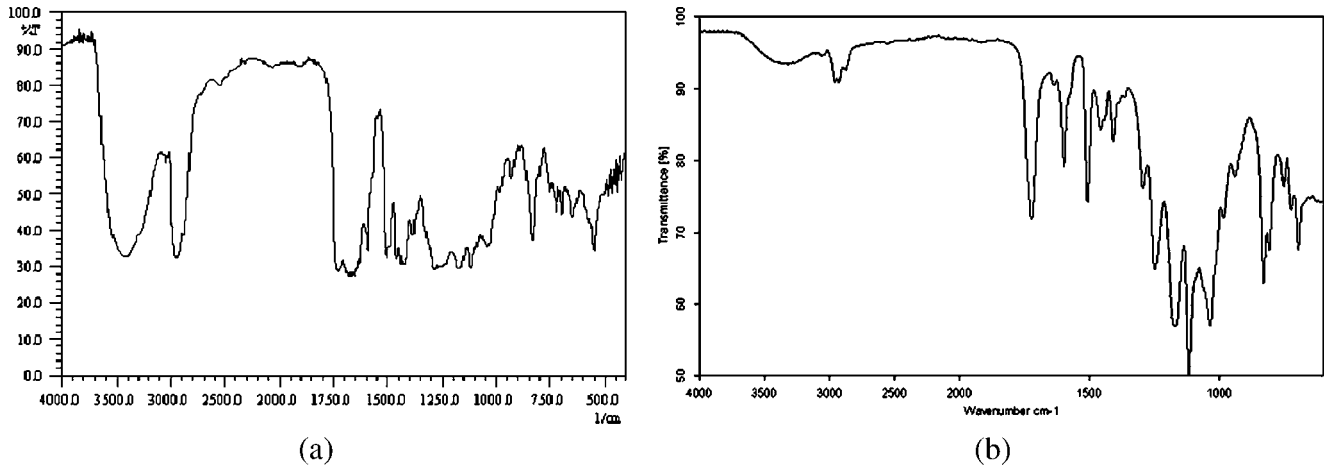


**Figure 4** (a) FTIR Spectrum of 10 wt % hybrid coating as control and (b) ATIR of the 10 wt % hybrid coating on Al surface.

can be seen that the EC (Erichson cupping test) values are in between 2.3 and 1.2 mm. The hybrid coating with 30% sol–gel precursor content has pendulum hardness value of 274 s and flexibility 1.2 mm. From this result, it can be concluded that hybrid coatings show a trend toward a very hard but much less flexible system. Compared with pure organic coating, flexibility of all hybrids decreased as a function of sol–gel percentage.

Figure 6 shows impact resistance of samples as a function of sol–gel precursor. The force needed to crack the film was measured as impact strength. As can be seen in Figure 6, the impact strength of all hybrid materials are higher than the corresponding value found in pure organic coating. This would indicate that hybrid films tend to be harder and less flexible as the precursor content was increased.

The thermal stability of the hybrid coatings was investigated with thermogravimetric analysis. Figure 7 shows the TGA thermograms of the hybrids in air atmosphere. The analyzing data was collected in Table III. One can see that all samples exhibited a 5% weight loss at around 160°C followed by a rapid loss over the temperature range from 380 to 440°C. Gas chromatography/mass spectrometry (GC-MS) was used to identify volatile and semivolatile organic compounds generated by the thermal degradation reaction at low temperatures and the results will be discussed later. The weight loss at higher temperature is probably due to the cleavage of polymer chain and further oxidation of silicates. The onset of weight loss is almost the same for all coatings independent of the phosphorus and silica contents. Maximum decomposition temperature of pure organic

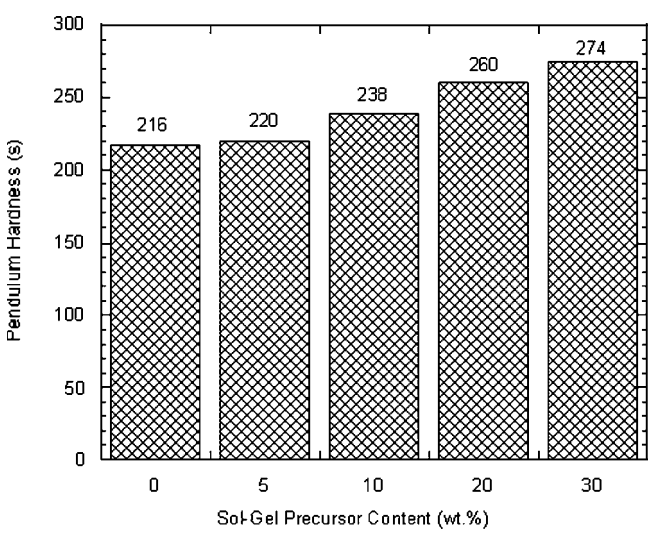


**Figure 5** The effect of sol–gel precursor content on the pendulum hardness of hybrid coatings.

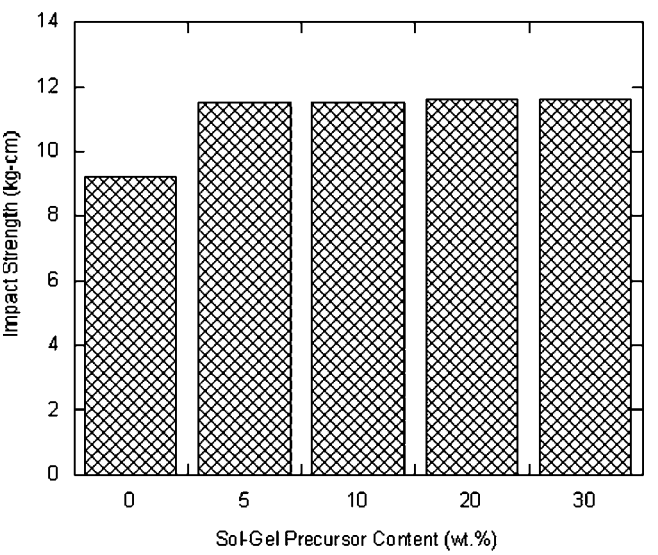


**Figure 6** The effect of sol–gel precursor content on the impact resistance of hybrid coatings.

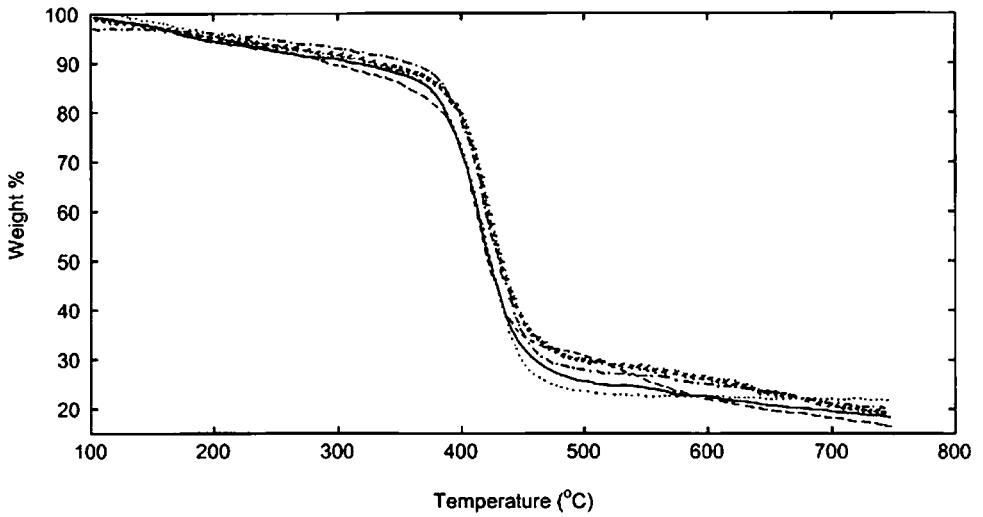


**Figure 7** Weight loss versus temperature as a function of sol–gel precursor content (------, CONTROL; ———, PPCH1; ....., PPCH2; -.-.-.-.-., PPCH3; xxxxxx, PPCH4).

coating is 417°C. This weight loss could be ascribed to the decomposition of the phosphorus groups that caused the formation of the phosphorus-rich residues. The char yield is 17% at 750°C for pure organic coating. It is known that a high char yield can usually limit the production of combustible carbon-containing gases and decrease the thermal conductivity of the surface of a burning material. Therefore, flammability of the material is reduced.[26] Incorporation of inorganic part (up to 20%) into the organic network increases the maximum weight loss temperature to 424°C. This would indicate that, the covalent bonds between organic and inorganic networks could improve the thermal stability. In addition, the char yield of pure organic coating is higher than that of all hybrid coatings at 500°C. This observation shows that, a decreasing percentage of phosphorus containing acrylate oligomer with increasing silica sol content in hybrid coating lowers the char yield at 500°C. However, by further increase in temperature (750°C), one can see clearly the effect of hybrid structure on flame retardancy. Moreover, it should be noted that all the char yield values reported in this work are much higher than our previous study in which the best value was 4.6% in the absence of APPO oligomer at 750°C.[27]

The GC-MS studies were performed at four different temperatures between 50 and 150°C for all samples. No thermal degradation product can be found below 100°C. Above this temperature, very similar profiles were obtained. Figure 8 displays the GC-MS spectrum recorded for 20 wt % of hybrid coating at 125°C. At GC-MS analyses showed that the initial weight loss in Figure 7 is due to the degradation products of unreacted photoinitator and reactive diluent. The presence of peaks at 16.79 min [*m/z*: 77 (phenyl), 105 (benzoyl), 106 (benzaldehyde)], at 22.28 min [*m/z*: 98 (1-hydroxy cyclohexyl)], and at 30.62 min [*m/z*: 99 (cyclohexanol)], derived from cleavage of the Irgacure 184, proved this occurrence. In addition, peaks corresponding to fragments of *N*-vinyl pyrrolidone [*m/z*: 85 (2-pyrrolidone) at 18.48 min and 111 (*N*-vinyl pyrrolidone) at 19.31 min] can also be detected. The peak observed at 7.94 min (*m/z*: 49) corresponds to residual dichloromethane, which is used in oligomer synthesis.

**TABLE III**
**TGA Analysis of Hybrid Films**

| Sample | APPO wt % in hybrid coating formulation | 5% Weight loss temperature, $T_d$ (°C) | Max weight loss temperature (°C) | Residue (%) | | |
|---|---|---|---|---|---|---|
| | | | | 500°C | 600°C | 750°C |
| Control | 25 | 153 | 417 | 32 | 23 | 17 |
| PPCH1 | 24 | 155 | 421 | 26 | 23 | 19 |
| PPCH2 | 23 | 167 | 423 | 24 | 23 | 22 |
| PPCH3 | 21 | 159 | 424 | 28 | 26 | 20 |
| PPCH4 | 19 | 170 | 423 | 30 | 27 | 19 |

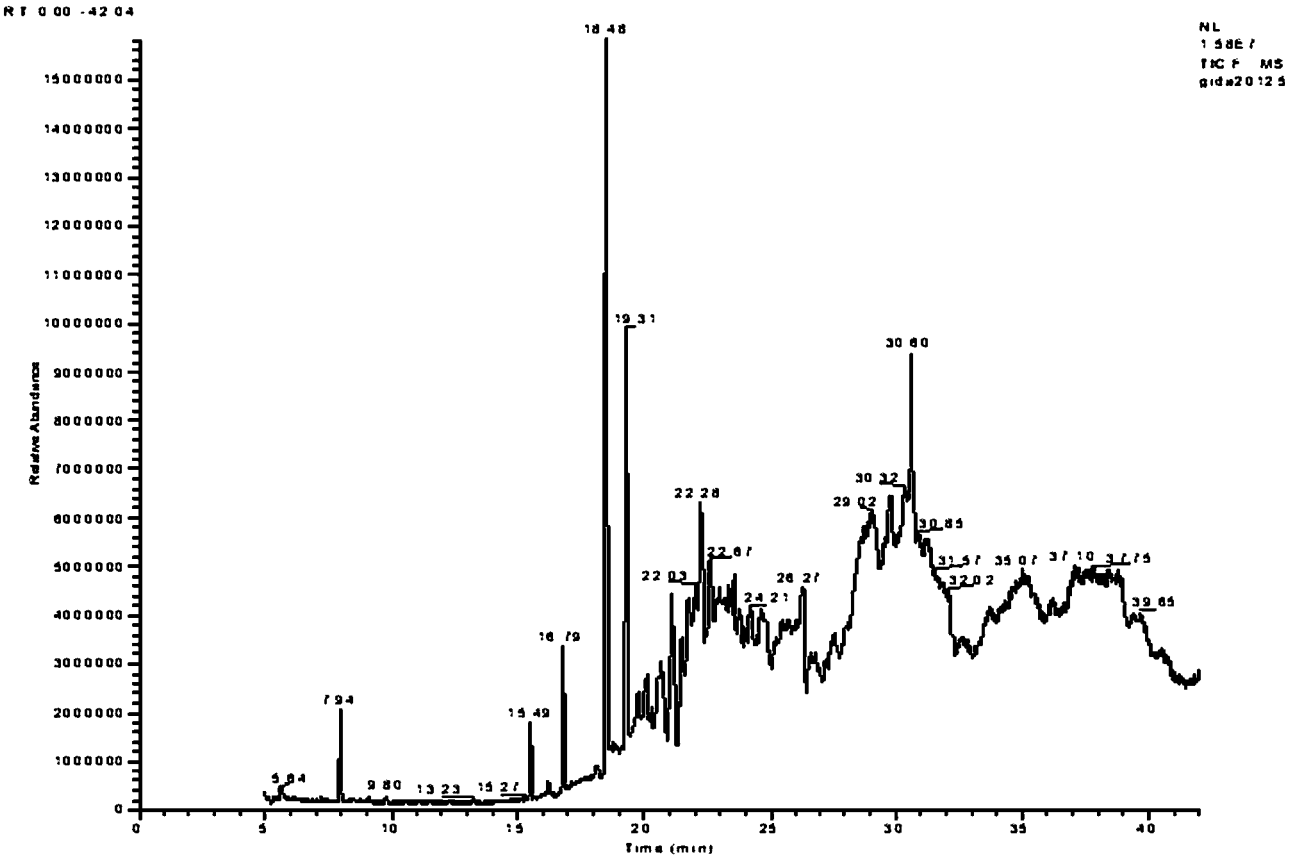


**Figure 8** GC-MS chromatograms of 20 wt % hybrid coating at 125°C.

In conclusion, under the evaluation of all results, the best coating may be chosen as PPCH3 with respect to its appearance, hardness, thermal stability, and flame retardant behaviors.

## CONCLUSIONS

In this article, a series of UV-curable organic–inorganic hybrid coatings were prepared based on sol–gel reactions for TEOS and MAPTMS in the presence of acrylated phenylphosphineoxide resin (APPO) and a bisphenol-A-based epoxy acrylate resin. The $^{29}$Si CP/MAS NMR spectrum of the 10 wt % of hybrid sample showed that the hydrolysis and condensation reactions of MAPTMS and TEOS structures have proceeded very rapidly and almost fully condensed structure was obtained. Incorporation of TEOS and MAPTMS greatly improves the hardness of pure acrylate-functionalized organic coating. Upon increasing the inorganic content, the other properties such as gloss, adhesion, and impact strength are also improved. The composition of the organic phase in the sol–gel matrix can be used to optimize the flame-retardant properties of hybrid coating. Incorporation of phosphorus containing oligomer into the organic part strongly increased flame resistance of hybrid samples.

The authors are pleased to acknowledge WACKER and BASF for their kind support by providing the chemicals.

## References

1. Haas, K. H.; Walter, H. Curr Opin Solid State Mater Sci 1999, 4, 571.
2. Mark, J. E.; Jiang, C.; Tang, M. Y. Macromolecules 1984, 17, 2616.
3. Brennan, A. B.; Wilkes, G. L. Polymer 1991, 32, 733.
4. Landry, C. J. T.; Coltrain, B. K.; Wesson, J. A.; Zumbulyadis, N.; Lippert, J. L. Polymer 1992, 33, 1496.
5. Mackenzic, J. D.; Bescher, E. J Sol Gel Sci Technol 2003, 27, 7.
6. Latella, B. A.; Ignat, M.; Barbe, C. J.; Cassidy, D. J.; Barlett, J. R. J Sol Gel Sci Technol 2003, 26, 765.
7. Chiang, C. L.; Ma, C. C.-M. Eur Polym J 2002, 38, 2219.
8. Chou, T. P.; Chandrasekaran, C.; Limmer, S. J.; Seraji, S.; Wu, Y.; Forbess, M. J.; Nguyen, C.; Cao, G. Z. J Non-Cryst Solids 2001, 290, 153.
9. Buestrich, R.; Kahlenberg, F.; Popall, M.; Dannberg, P.; Muller-Fiedler, R.; Rösch, O. J Sol Gel Sci Technol 2001, 20, 181.
10. Innocenzi, P.; Brusatin, G. J Non-Cryst Solids 2004, 333, 137.
11. Soppera, O.; Croutxe-Barghorn, C.; Carre, C.; Blanc, D. Appl Surf Sci 2002, 186, 91.
12. Messori, M.; Toselli, M.; Pilati, F.; Fabbri, E.; Busoli, S.; Pasquali, L.; Nannorone, S. Polymer 2003, 44, 4463.
13. Murata, H.; Chang, B.-J.; Prucker, O.; Dahm, M.; Rühe, J. Surf Sci 2004, 570, 111.
14. Bosch, P.; del Monte, F.; Mateo, J. L.; Levy, D. J Polym Sci Part A: Polym Chem 1996, 34, 3289.

15. Zhang, L.; Zeng, Z.; Yang, J.; Chen, Y. J Appl Polym Sci 2003, 87, 1654.
16. Hsiue, G.; Kuo, W. J.; Huang, Y. P.; Jeng, R. J. Polymer 2000, 41, 2813.
17. Wouters, M. E. L.; Wolfs, D. P.; van der Linde, M. C.; Hovens, J. H. P.; Tinnemans, A. T. A. Prog Org Coat 2004, 51, 312.
18. Bayramoğlu, G.; Kahraman, M. V.; Kayaman-Apohan, N.; Güngör, A. Prog Org Coat, to appear.
19. Smith, C. D.; Grubbs, H.; Webster, H. F.; Gungor, A.; Wightman, J. P.; McGrath, J. E. High Perform Polym 1991, 3, 211.
20. Riley, D. J. Ph.D. Thesis, Virgina Polytechnic Institute, 1997.
21. Liaw, D. J.; Chen, P.-S. J Polym Sci Part A: Polym Chem 1996, 34, 885.
22. Ni, H.; Simonsick, W. J., Jr.; Skaja, A. D.; Williams, J. P.; Soucek, M. D. Prog Org Coat 2000, 38, 97.
23. Martinez-Alonso, S.; Rustad, J. R.; Goetz, A. F. H. Am Mineralogist 2002, 87, 1215.
24. Bradbury, S. E.; Williams, Q. Am Mineralogist 2003, 38, 1460.
25. Soucek, M. D. Prog Org Coat 1999, 36, 89.
26. Chen-Yang, Y. W.; Lee, H. F.; Yuan, C. Y. J Polym Sci Part A: Polym Chem 2000, 38, 972.
27. Kahraman, M. V.; Kuğu, M.; Menceloğlu, Y.; Kayaman-Apohan, N.; Güngör, A. J Non-Cryst Solids 2006, 352, 2413.